Fatigue-crack propagation in Nitinol, a shape-memory and superelastic endovascular stent material

A. L. McKelvey, R. O. Ritchie
Department of Materials Science and Mineral Engineering, University of California, Berkeley, California 94720-1760

Received 28 January 1999; accepted 13 April 1999

Abstract: Improving the design and performance of medical stents for implantation in the human body is of current interest. This paper describes a study of fatigue-crack propagation behavior in the superelastic alloy Nitinol. Specifically, the objective of this work was to study the effect of environment on cyclic crack-growth resistance in an ~50Ni–50Ti (atom %) alloy and to provide the necessary data for the safe life prediction of Nitinol endovascular stents. The material selected for this study was heat treated such that it was superelastic at human body temperature; this was confirmed with monotonic uniaxial tensile tests. Characterization of fatigue-crack growth rates was performed at 37°C on disk-shaped compact-tension samples in environments of air, aerated deionized water, and aerated Hank's solution (a simulated body fluid). The effect of cyclic loading on the uniaxial constitutive behavior was investigated at a strain range of 6.4%, and results indicate that the magnitude of available superelastic strain (~5.0%) is maintained even after cyclic softening. However, despite the persistence of nucleating the stress-induced martensitic phase after cycling with a maximum strain slightly below the plastic yield point, Nitinol was found to have the lowest fatigue-crack growth resistance of the principal metallic alloys currently used for implant applications. © 1999 John Wiley & Sons, Inc. J Biomed Mater Res, 47, 301–308, 1999.

Key words: Nitinol; stent; fatigue; shape-memory; superelastic

INTRODUCTION

There has been increasing interest in the biomedical industry to improve the design and performance of medical stents for implantation in the human body. In this regard, the titanium-based alloy Nitinol has become an attractive replacement for the currently used material, stainless steel, due to Nitinol's improved corrosion resistance in physiological environments, interesting nonlinear mechanical behavior, and its thermoelasticity. Despite this interest in implementing the use of Nitinol stents, little is known about their mechanical performance. Indeed, there is considerable activity to develop other medical devices using Nitinol as well, yet these endeavors, too, are limited by the current lack of understanding of the structural properties of Nitinol alloys. In particular, this makes such critical tasks as stress analysis and life prediction somewhat uncertain. Moreover, although the simple tension and compression properties of Nitinol are reasonably well characterized, there is very little understanding of, or engineering data on, its fracture and cyclic fatigue behavior. Accordingly, there is a critical need for materials science studies that will give us an understanding of such vital topics as stress analysis, constitutive behavior, fracture, fatigue, and life prediction for medical implant devices involving superelastic materials.

This study examines the fatigue-crack propagation behavior of superelastic Nitinol, specifically focusing on the role of a simulated physiological environment on crack-growth rates in this alloy.

Correspondence to: R.O. Ritchie
Contract grant sponsor: Nitinol Devices and Components, Inc., Fremont, California

 CCC 0021-9304/99/030301-08

Superelastic effect of Nitinol

Nitinol is a titanium-based thermoelastic material with a composition of approximately 50 atomic % nickel, which originally gained fame during the 1960s for its shape-memory behavior (Fig. 1).[1,2] This effect is a result of an athermal martensitic transformation that occurs over a particular temperature range by a uniform lattice shear without a change in the material's composition. Although the shape-memory effect is interesting, it has little to do with stent design. Subsequent discussion will focus on the more relevant stress-induced superelastic transformation.

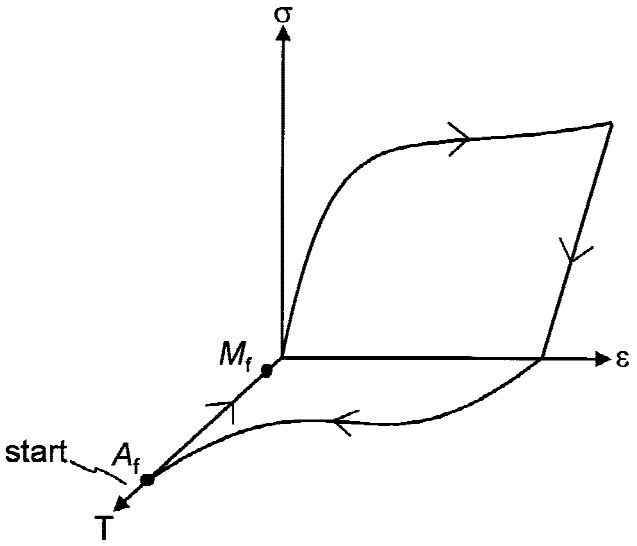

Figure 1. Schematic illustration of the shape-memory effect. An austenite sample is cooled through the martensitic transformation to a temperature below the martensite finish temperature, M_f. At this point the sample is deformed to within ~10% strain. After unloading, the sample is heated through the martensite to austenite transformation. The martensite laths revert to austenite along the original paths, such that the deformation previously applied disappears as the temperature is increased. At A_f the strain is completely recovered, and the material has the same original shape before the deformation portion of the cycle. This is a result of the material's thermoelasticity, low symmetry martensite crystal structure, and also due to the role of twinning in the martensite phase.

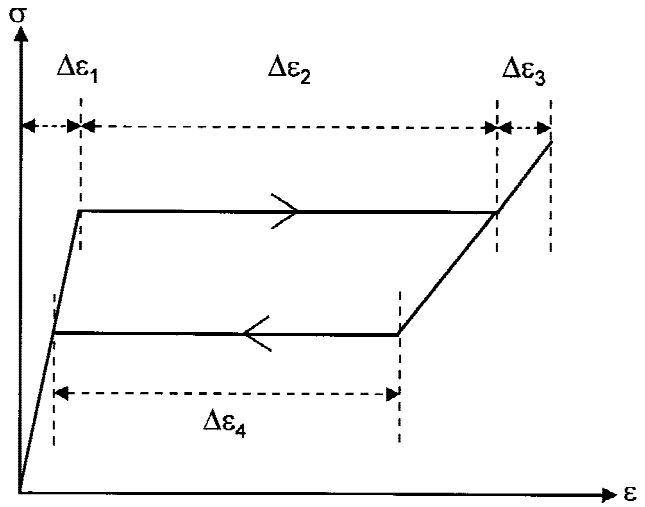

Figure 2. Schematic illustration of the superelastic effect. The first elastic deformation shows a large stress increase over a small strain range, $\Delta\varepsilon_1$. Following this initial deformation, the curve plateaus, with little change in stress for a much larger strain range, $\Delta\varepsilon_2$. On this plateau, martensite laths nucleate and grow with the preferred martensite variant. After the martensitic transformation is complete, elastic deformation continues over the strain range, $\Delta\varepsilon_3$, until yielding of the martensite or unloading. When the stress is decreased, the reverse process is observed. After elastic recovery over $\Delta\varepsilon_3$ (and an additional small strain increment before the lower plateau is reached), the plates that formed during loading over $\Delta\varepsilon_2$ revert along the previous crystallographic path, and, hence, the volume fraction of martensite decreases over $\Delta\varepsilon_4$. This is the process by which the parent phase is recovered so that the original undeformed material is restored.

Nitinol alloys can exhibit superelasticity at temperatures slightly above the austenite finish temperature, A_f. The superelastic effect is attributed to a reversible stress-induced martensitic transformation (Fig. 2). The stress–strain hysteresis is characterized by three distinct parts. The first elastic distortion shows a large stress increase over a small strain range, $\Delta\varepsilon_1$. Following this initial deformation, the curve plateaus with little change in stress for a much larger strain range, $\Delta\varepsilon_2$. On this plateau, martensite laths nucleate and grow with the preferred martensite variant, that is, the one most compliant with respect to the tensile axis. [The monoclinic martensite phase in Nitinol forms in plate groups where four variants with habit plane (551) cluster about six <011> poles, resulting in 24 possible variants.[3]] After the martensitic transformation is complete, elastic deformation continues over the strain range, $\Delta\varepsilon_3$, until yielding of the martensite or unloading. When the stress is decreased, the reverse process is observed. After elastic recovery over $\Delta\varepsilon_3$ (and an additional small strain increment before the lower plateau is reached), the plates that formed during loading over $\Delta\varepsilon_2$ revert along the previous crystallographic path and, hence, the volume fraction of martensite decreases over $\Delta\varepsilon_4$. This is the process by which the parent phase is recovered, so the material is returned to its nondeformed configuration. The temperatures at which these described transformations occur can be carefully controlled by manipulating the composition, prior cold work, heat treatment, and cooling rate during quenching.[4]

Nitinol for stents

Superelastic stents offer an improved alternative over current options for constricted coronary and carotid arteries. Balloon angioplasty is a technique often used in place of by-pass surgery. The balloon is inserted into the vascular system remotely (e.g., via the femoral artery) and inflated at the blocked arterial site. In order to compress the plaque and open the constriction, usually the balloon must be inflated to ~12 atmospheres of pressure. This can induce damage to the vessel wall and cause the artery to be more compliant and susceptible to failure.[5] Stenting is similar to balloon angioplasty as the surgery is noninvasive; however, it has the additional advantage that it provides a rigid, permanent support in the artery that reduces the risk of repeated operations. The stent is simply a hol-

low tube or helical wire designed to support the vessel walls and permit blood circulation through the blockage. Since the stent is permanently left in the body in a fixed position, the risk of arterial collapse is avoided. Currently the vast majority of stents are manufactured from stainless steel; however, titanium and tantalum stents have been proposed[6] and are being developed. Application of these devices requires expanding the stent beyond the plastic limit of the alloy such that it permanently deforms and embeds in the arterial wall. This plastic deformation can greatly reduce the fatigue life of the stent and therefore make it more susceptible to failure *in vivo*.

A dramatic advantage Nitinol has over other alloys is its enhanced recoverable elastic strain. While stainless steel has approximately 0.5% available elastic strain, Nitinol has ~8% due to its superelastic transformation (Fig. 2). Nitinol stents would be inserted into the body, similar to stainless steel stents, except they would be self-expanding as a result of the superelastic effect. Because they need not be embedded into the arterial wall by permanent deformation, it is expected that Nitinol stents would have longer fatigue lives and that the risk of failure would be greatly reduced.

Another advantage Nitinol has in stent applications is its *biased stiffness*[7] (Fig. 3). When open, the stent is in its relaxed state by design. As the stent is compressed into a guide catheter, the device is loaded up the superelastic plateau. After the stent is deployed, it opens and the stress is reduced to a value along the unloading plateau. While a gentle pressure is maintained to keep the artery open, any contraction, or blood vessel diameter reduction, would result in a higher resistance to loading and therefore giving rise to biased stiffness. This is a result of the different loading and unloading paths in the monotonic constitutive behavior.

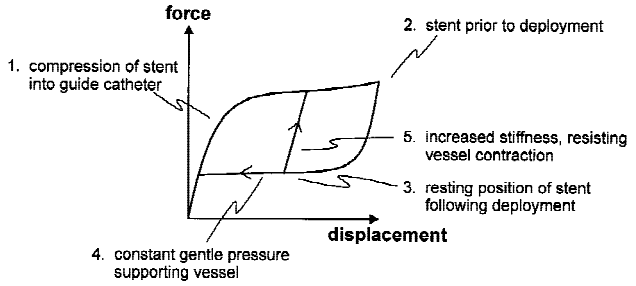

Figure 3. Schematic illustration of the advantage of biased stiffness in Nitinol (after Duerig et al.)[7]. The relaxed state of the stent is open. As the stent is compressed into a guide catheter, the force increases. When the stent is deployed at the location of the constriction, the force decreases along the unloading plateau. The blood vessel is supported by constant gentle pressure; however, the resistance to future constriction is enhanced by the distinct loading curve with greater stiffness.

Motivation for fatigue characterization

Although Nitinol stents offer many advantages compared to current designs, it is critical that these components not suffer mechanical failure *in vivo*. It is widely recognized that cracks always exist in materials and that components must be tolerant of their presence. Fracture mechanics provides a basis for design in the presence of such cracks, using damage-tolerant concepts. This approach is particularly relevant for stents, which often are fabricated by laser machining. This process invariably leaves a distribution of small (5 to 20 μm-sized) cracks in the surface. However, despite the obvious need for such approaches from an engineering perspective, damage-tolerant design methodologies rarely have been implemented in the biomedical industry. One example known is that of pyrolytic-carbon mechanical heart valves, where critical crack sizes, fatigue life, and fracture toughness data have been incorporated into the valve design and fabrication.[8] Damage-tolerant design is actively used in other industries (e.g., the aerospace technology) to estimate failure load/critical crack size combinations essential for the prediction of a component's mechanical life.

Although the thermodynamics and phase transformations of the shape-memory and superelastic effects have been widely studied, currently there are only very limited data in the literature that describe crack propagation in Nitinol alloys under monotonic or cyclic loading.[9–11] Furthermore, none of the data in these studies characterizes the fatigue behavior of *superelastic* Nitinol. In stents, cyclic loads would arise from the difference in systolic and diastolic blood pressures and from the stress associated with the contraction of the heart muscle (e.g., in coronary stents). Often in other structural components, the safe life is governed by the time it takes incipient crack to *propagate* to failure. However, in the case of stents, the width of a strut is very fine (e.g., ~250 μm), and therefore the design may be limited to the fatigue threshold, ΔK_{TH}, which describes the stress-intensity range for the onset of crack propagation. Thus, it is critical that the crack-propagation rates, and in particular the threshold ΔK_{TH} values, in superelastic NiTi are known in order to estimate expected device lifetimes and to provide a rational design against fatigue failure.

The superelastic transformation in Nitinol is a potential source of resistance to fracture and fatigue. Mechanically induced phase transformations already have been exploited as a method for increasing the fracture toughness in several materials.[12] Stress-induced martensitic transformations are known to occur in austenitic steels and TRiP steels.[13,14] Also, transformation toughening is observed in brittle materials, which greatly enhances their fracture toughness.[15–21] For example, in partially stabilized ZrO_2, metastable

coherent tetragonal particles are dispersed throughout a cubic matrix.[21] When a tensile stress is applied, the metastable tetragonal particles undergo a martensitic phase transformation to a monoclinic crystal structure. This phase transformation increases the volume of the particles, which at a crack tip reduces the local stress intensity, shielding the tip from the applied load.

Studies on the fatigue of austenitic stainless steels[14–22] and partially stabilized zirconia ceramics[23] have shown that in the presence of an *in situ* phase transformation, resistance to crack advance can be enhanced significantly. However, in both the latter examples, the transformation involved a significant and positive dilatational component, which, due to the constraint of surrounding elastic (untransformed) material, resulted in crack extension into a zone of compressed material.[24,25] Conversely, the transformation in Ti-Ni alloys largely involves pure shear with only a small, *negative* volume change,[9] and therefore it is not known if the micromechanisms that contribute to fracture resistance in Nitinol are similar.

EXPERIMENTAL METHODS

The Nitinol material studied had a composition of 55 Ni–45 Ti (wt %) and was received in the form of a 41.3 mm in diameter round bar. Disk-shaped compact tension samples were electro-discharge machined to have dimensions of 31 mm in width and 9 mm in thickness. These disks were heat treated in air at 500°C for 35 min and then rapidly quenched in an ice water bath. Fatigue tests were conducted at 37°C in air, aerated deionized water, and aerated Hank's solution (a simulated physiological environment) under automated stress-intensity control on electro-servo hydraulic machines at 10 Hz (sine wave), in general accordance with the testing techniques described in ASTM E647. Samples were cycled at a load ratio (R) equal to 0.1, where R is defined as the ratio of the minimum to the maximum stress intensities in the loading cycle (i.e., $R = K_{min}/K_{max}$). The testing temperature of 37°C was monitored using either a Teflon-coated probe in aqueous environments or a surface-resistive-temperature device in air with the temperature maintained to within ±0.2°C. Samples tested in air were heated via infrared heat lamps whereas samples tested in aqueous solution were heated via a Teflon-coated heating element. The composition of Hank's solution, which had a pH of 7.4, was (in g/L): 0.185 calcium chloride/$2H_2O$; 0.09767 magnesium sulfate (anhydrous); 0.4 potassium chloride; 0.06 potassium phosphate monobasic (anhydrous); 8.0 sodium chloride; 0.04788 sodium phosphate dibasic (anhydrous); 1.0 D-glucose; and 0.35 sodium bicarbonate.

Round-bar uniaxial tensile samples with gauge dimensions of 25.4 mm in length and 6.40 mm in diameter were also heat treated in air at 500°C for 35 min before being rapidly quenched in an ice water bath. Monotonic- and cyclic-tensile tests were conducted under displacement control at a rate of 2.5 μm/s, which corresponds to a strain rate of ~1×10^{-4} /s for the selected gauge length. The monotonic and cyclic constitutive behavior was measured at 37°C; samples were heated in a warm distilled water bath (minimal corrosion effects were expected with this environment in Nitinol[26]), with the sample temperature again maintained to within ±0.2°C.

RESULTS AND DISCUSSION

Monotonic constitutive behavior

In order to demonstrate that the material was superelastic, the residual permanent set, or lack thereof, was measured on a sample loaded to greater than 1% strain. This test was conducted at 37°C on a sample arbitrarily displaced to ~4.5% strain and then unloaded (Fig. 4). The alloy displayed linear elastic distortion until the critical stress (~407 MPa) to nucleate martensite in the material was applied (Fig. 4). The volume fraction of martensite increased along the loading plateau until it was unloaded at ~4.5% strain; next, the stress decreased to ~200 MPa, at which point

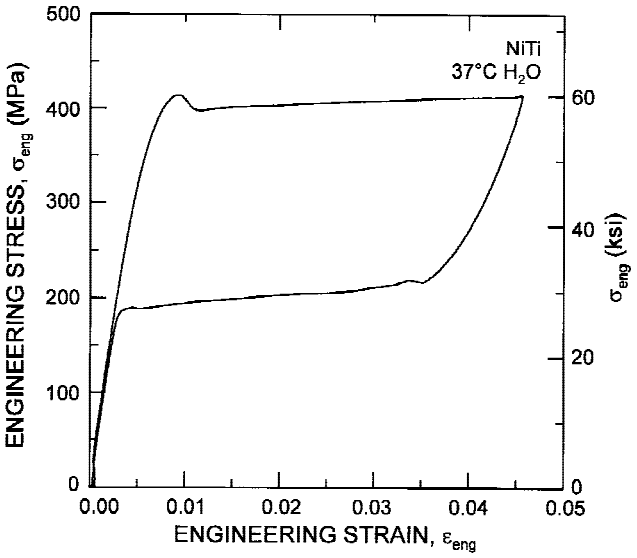

Figure 4. A plot of results that verified that NiTi was superelastic at 37°C after the material had been heat treated at 500°C for 35 min in air followed by an ice water quench. The material displayed linear elastic distortion until the critical stress to nucleate martensite in the material was applied (~407 MPa). The volume fraction of martensite increased along the loading plateau until the sample arbitrarily was unloaded at ~4.5% strain. At ~200 MPa, the volume fraction of martensite began to decrease along the lower plateau. After complete unloading, there was no detectable permanent strain, and, hence, the material was superelastic.

the volume fraction of martensite decreased along the lower stress plateau. After complete unloading, there was no detectable permanent strain, and hence the transformation was superelastic and geometrically reversible. The complete uniaxial constitutive behavior at 37°C is shown in Figure 5. The alloy displayed a loading stiffness of 62 GPa until the critical stress (~407 MPa) to nucleate martensite in the material was applied. The volume fraction of martensite increased along the loading plateau to approximately 5% strain, at which point the transformation was presumed to be nearly complete and the stress began to increase again with a loading stiffness of 22 GPa. The 0.2% offset plastic yield point from the second linear elastic region was found to be 1058 MPa at a strain of 8.2%. The strain-to-failure was 21.3% (for a 25.4 mm gauge length).

Effect of environment on fatigue-crack growth behavior

In order to develop an understanding of fatigue-crack growth behavior in Nitinol it is necessary to examine crack-growth rates in a relatively inert environment as well as in a simulated body fluid. Accordingly, fatigue-crack propagation rates were measured (at 37°C) at 10 Hz, with an R of 0.1, in air as well as in aerated deionized water and aerated Hank's solution. While it is unclear whether an endovascular stent may be subjected to an aerated or deaerated environment *in vivo*, the aqueous solutions selected for this study were aerated in order to examine the "worst-case" condition. Results are shown in Figure 6. From these data it is clear that a significant effect of corrosion fatigue is not apparent in Nitinol at the frequency studied (10 Hz) in Hank's solution as growth rates are essentially identical to those measured in air and aerated deionized water. Note that while deionized water is seemingly inert, dissolved oxygen in neutral pH solutions is known to be a corrosive species in fatigue-crack growth of metals.[27] Thus, despite the presence of oxygen in the aerated solutions and chloride ions in the Hank's solution, the fatigue-crack growth behavior in Nitinol appears to be unaffected.

To predict the lifetime of a Nitinol medical device, it is generally necessary to obtain an empirical fit to such fatigue-crack growth data. The simplest approach is to use a Paris power-law-like formulation, that is, $da/dN = C\Delta K^m$, where da/dN is the crack growth rate per cycle, C is a constant, ΔK is the applied stress-intensity range, and m is the Paris exponent. This equation is then integrated and solved in terms of N, the number of cycles until failure, by substituting initial and final crack lengths. For Nitinol, a threshold ΔK_{TH} of 2 MPa√m is seen, with a Paris exponent in the mid-growth regime of m~3; the stress intensity range at

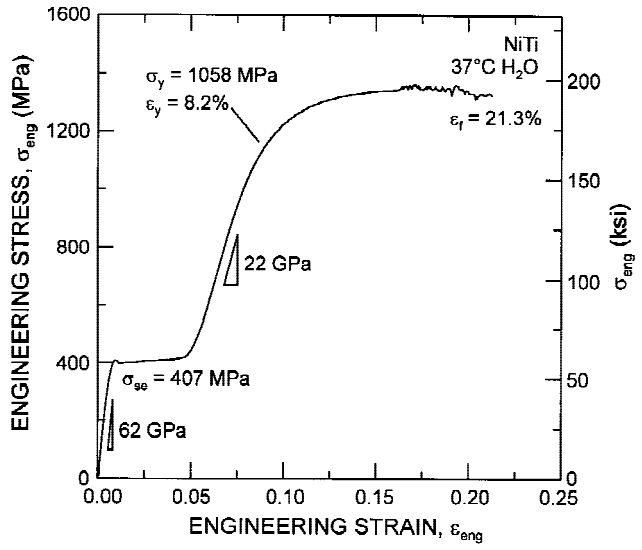

Figure 5. The complete uniaxial constitutive behavior in NiTi at 37°C is shown. The alloy displayed an initial loading stiffness of 62 GPa until the critical stress (~407 MPa) to nucleate martensite in the material was applied. The volume fraction of martensite increased along the loading plateau to approximately 5% strain. With further displacement, a new loading stiffness of 22 GPa was observed until general yielding began at 8.2% strain and 1058 MPa. The strain-to-failure was 21.3% for a gauge length of 25.4 mm.

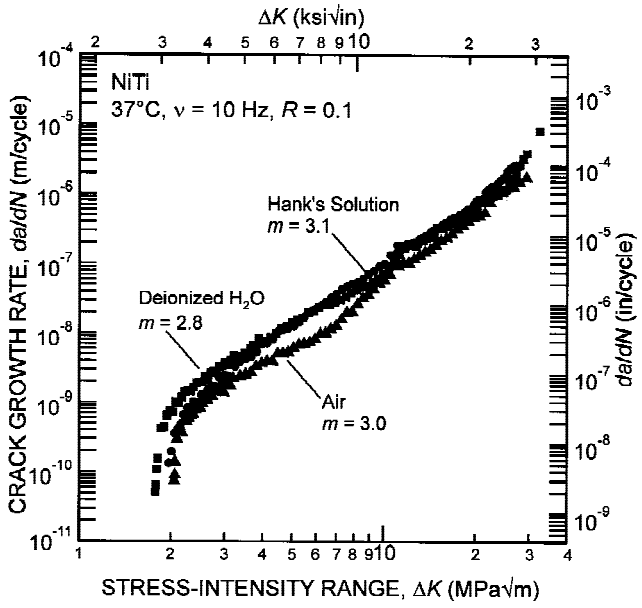

Figure 6. A plot showing the effect of environment on crack-growth rates in superelastic Nitinol. Data were collected at 37°C, R = 0.1, 10 Hz in air, aerated deionized water, and aerated Hank's solution, a simulated body fluid. All three data sets were similar, with the threshold for fatigue-crack propagation ~2 MPa√m, the slope of the mid-growth regime (or Paris exponent m) approximately 3, and the maximum applied stress-intensity range prior to fatigue failure and fast fracture ~30 MPa√m.

instability prior to failure is approximately ΔK~30 MPa$\sqrt{m}$.

Effect of cyclic loading on superelasticity

As Nitinol stents would be subjected to variable loads, the lack of degradation of the superelastic effect with cycling must be investigated and confirmed. Accordingly, the cyclic constitutive behavior has been measured for a large strain amplitude corresponding approximately to the limit of the superelastic plateau. The cyclic stress–strain response for an initial strain range of $\Delta\varepsilon$ = 6.4% is shown in Figure 7. The data plotted include the constitutive behavior for the 1st, 10th, 50th, and 100th cycles. The material was found to display cyclic softening where the stress required to nucleate the martensitic phase transformation and the peak stress at the maximum strain in the displacement range decreased with repeated cycling. It is clear that the rate of change in the constitutive relationship decreases with increasing numbers of cycles [Fig. 7(a)]; for instance, the magnitude of cyclic softening is largest between the 1st and 10th cycles while there is little difference between the 50th and 100th cycles. Furthermore, the permanent set, or residual plastic strain, was found to be saturated after approximately 60 cycles [Fig. 7(b)], whereupon it remained relatively constant at a value of 2.1% with continued deformation. This is believed to indicate that the microstructure has been "saturated" (i.e., negligible further changes in dislocation/twinning structure) for the given strain range applied. It is important to note that after saturation, the magnitude of reversible superelastic strain is still on the order of 5%. While these results are preliminary—the complete cyclic stress–strain behavior over a variety of strain ranges is necessary and under current investigation—these data do indicate that the material remains superelastic with reversible strains of ~5% after repeated loading below the plastic yield point, which in this material is ~1058 MPa (Fig. 5).

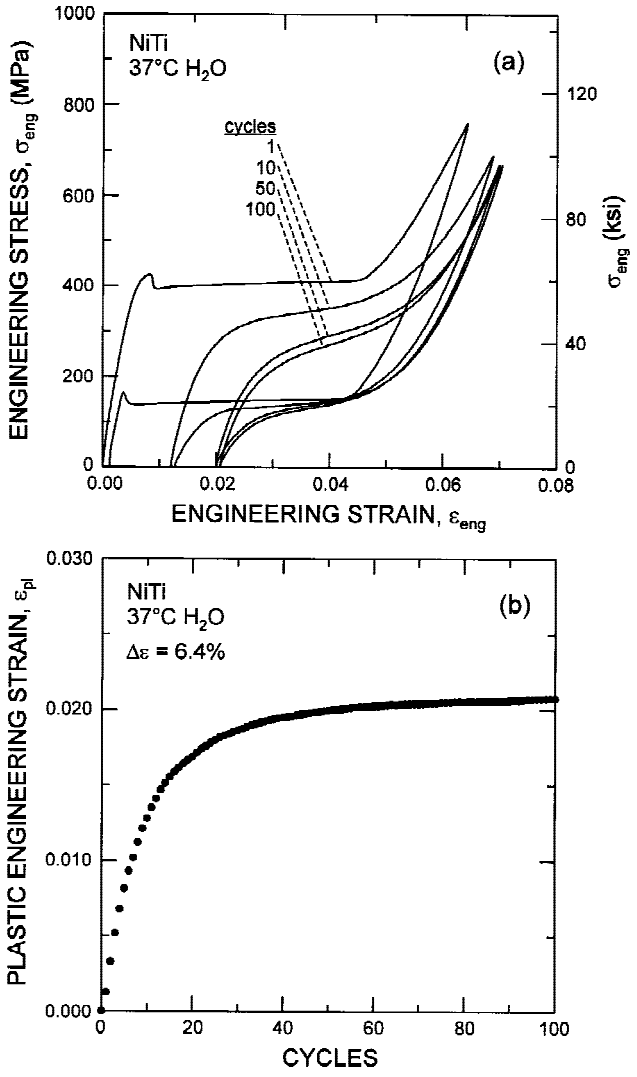

Figure 7. A plot of the cyclic constitutive behavior in Nitinol. (a) At 37°C in distilled water at a strain rate of ~1 ×10^{-4}/s. The data shown are from the 1st, 10th, 50th, and 100th cycles. The change in permanent set, or plastic residual strain, is shown in (b), where saturation appears after ~60 cycles.

Comparison of fatigue-crack propagation with other biomedical alloys

While the absence of corrosion fatigue in Nitinol (at least at 10 Hz) and the persistence of the superelastic effect after cyclic loading are encouraging, it must be emphasized that the threshold ΔK_{TH} values, below which fatigue-crack growth is presumed dormant, were found to be very low for Nitinol when compared to other metallic structural materials used for biomedical implants. To demonstrate this point, Figure 8 is a plot of the fatigue-crack growth rates for Nitinol from this study compared with other biomedical metallic alloys, namely, stainless steel, pure titanium, Ti-6Al-4V, and a CoCr alloy. Although these data are for moist air environments rather than for simulated body fluid, the fatigue threshold was the lowest and the crack-growth rates were the fastest in Nitinol. Specifically, ΔK_{TH} is ~4 MPa$\sqrt{m}$ in a Ti-6Al-4V alloy,[28] which is a factor of ~2 greater than the NiTi fatigue threshold. Type 316L stainless steel[29] has a ΔK_{TH} equal to 6 MPa$\sqrt{m}$, and the maximum applied stress-intensity range prior to failure is nearly 70 MPa$\sqrt{m}$. The largest differences in ΔK_{TH} compared to Nitinol, however, are for the remaining alloys on Figure 8. The fatigue threshold for a cobalt–chrome alloy, Haynes 25, which is used in many biomedical applications, including

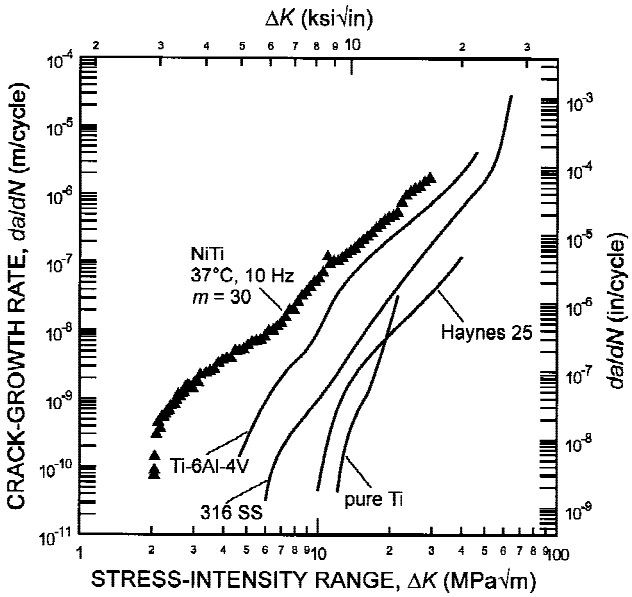

Figure 8. Comparison of fatigue-crack growth rates for various biomedical metallic alloys. Data for NiTi from present study; Ti-6Al-4V by Boyce and Ritchie, 1998, obtained at 25°C, 50 Hz, R = 0.1, m = 4.3; CoCr Haynes 25 alloy by Ritchie and Lubock, 1986, obtained at room temperature, 30 Hz, m = 3.5; 316L stainless steel by Pickard et al., 1975, obtained at 22°C, 100 Hz, R = 0.3, m = 4.9; and pure Ti by Li and Thompson, 1999, obtained at 25°C, 10 Hz, R = 0.1, m = 9.6. All tests were conducted in air.

cardiac valve prostheses, at R = 0.05, is ~10 MPa√m[30]—an increase factor of ~5 compared to ΔK_{TH} for NiTi. Furthermore, commercially pure Ti[31] has a fatigue threshold greater than 10 MPa√m when tested in air at room temperature. It should be noted, however, that several of these alloys show a reduction in their thresholds in corrosive environments whereas Nitinol appears to be far less susceptible to such effects.

This comparison of fatigue-crack threshold data may be quite relevant, as mentioned earlier, for the architecture of endovascular stents can be very fine. Therefore, it may be necessary to design such stents for fatigue resistance based on the threshold ΔK_{TH} to prevent any crack propagation since the component size is so small that a crack, once initiated, readily would traverse the entire stent cross section.

CONCLUSIONS

Based on a study of the cyclic constitutive and fatigue-crack growth behavior of a superelastic 55 Ni–45 Ti (wt %) Nitinol alloy at 37°C in air, aerated deionized water, and aerated Hank's solution (a simulated body fluid), the following conclusions can be made:

1. Fatigue-crack growth rates in Nitinol at a frequency of 10 Hz were found to be essentially identical in air, aerated deionized water, and aerated Hank's solution, suggesting that at this frequency, any environmentally assisted contributions to crack growth are minimal. Specifically, the threshold for the onset of fatigue-crack growth, ΔK_{TH}, was equal to ~2 MPa√m for all three environments. Furthermore, the slopes of the mid-growth regime, or Paris exponents m, were also similar and equal to ~3; the maximum applied ΔK at instability prior to failure was ~30 MPa√m for all three environments.
2. The cyclic stress–strain behavior investigated at an initial strain range equal to 6.4% revealed that the material's ability to undergo a stress-induced martensitic phase transformation is maintained. The alloy displayed cyclic softening, where the critical stress to nucleate the martensite phase and the peak stress at the limit of the strain range during loading decreased with increasing number of cycles. The rate of softening was found to decrease with further cycling. Saturation, as measured by the permanent set or residual strain after each incremental cycle, appeared after approximately 60 cycles, where the value of the permanent set reached a maximum value of 2.1% for the applied strain range.
3. Compared to other biomedical implant alloys, the fatigue-crack growth resistance of Nitinol was the lowest. Specifically, the ΔK_{TH} fatigue threshold value, at a fixed load ratio value of ~0.1, was significantly less by a factor between 2 and 5 than 316L stainless steel, pure Ti, Ti-6Al-4V, and a CoCr Haynes 25 alloy. Also, the crack-growth rates for any applied stress-intensity range were fastest in NiTi. These comparisons may cause concern as the architecture of endovascular stents, and of other medical devices, is quite fine, such that the onset of fatigue-induced cracking must be avoided completely if the structural integrity of the component is to be maintained.

Thanks are due to Drs. T. Duerig and A. Pelton of NDC for supplying the material and for useful discussions.

References

1. Buehler WJ, Wiley RC. Nickel-based alloys. US patent no. 3,174,851; 1965.
2. Jackson CM, Wagner HJ, Wasilewski, RJ. 55-Nitinol—The alloy with a memory: Its physical metallurgy, properties, and applications. NASA-SP 5110, National Aeronautics and Space Administration; 1972. 86 pp.
3. Saburi T, Wayman CM. Crystallographic similarities in shape memory martensites. Acta Metal 1979;27:979–995.
4. Wayman CM, Duerig TW. An introduction to martensite and shape memory. In: Duerig TW, Melton KN, Stockel D, Way-

man CM, editors. Engineering aspects of shape memory alloys. London: Butterworth–Heinemann Ltd.; 1990. p 3–17.
5. Chuter TAM, Donayre CE, White RA. Endoluminal vascular prostheses. Boston: Little, Brown and Company; 1995. 323 pp.
6. Bramfitt JE, Hess RL. A novel heat-activated recoverable temporary stent (HARTS system). In: Pelton AR, Hodgson D, Duerig T, editors. Proc. SMST-94: The first international conference on shape memory and superelastic technologies. Vol. 1. Monterey, California: MIAS; 1994. p 435–442.
7. Duerig TW, Pelton AR, Stockel D. The use of superelasticity in medicine. Metall 1996;50:569–574.
8. Ritchie RO. Fatigue and fracture of pyrolytic carbon: A damage-tolerant approach to structural integrity and life prediction in "ceramic" heart valve prostheses. J Heart Valve Dis 1996;5: S9–S31.
9. Dauskardt RH, Duerig TW, Ritchie RO. Effects of in situ phase transformation on fatigue-crack propagation in titanium–nickel shape-memory alloys. In: Otsuka K, Shimizu K, editors. Proc MRS International Meeting on Advanced Materials. Vol. 9. Pittsburgh: Materials Research Society; 1989. p 243–249.
10. Miyazaki S, Suizu M, Otsuka K, Takashima T. Effect of various factors on fatigue crack propagation rate in Ti-Ni alloys. In: Otsuka K, Shimizu K, editors. MRS International Meeting on Advanced Materials. Vol. 9. Pittsburgh: Materials Research Society; 1989. p 263–268.
11. Melton KN, Mercier O. Fatigue of NiTi thermoelastic martensites. Acta Metal 1979;27:137–144.
12. Ritchie RO. Mechanisms of fatigue crack propagation in metals, ceramics and composites: Role of crack tip shielding. Mater Sci Eng A 1988;103:15–28.
13. Olson GB, Cohen M. A general mechanism of martensitic nucleation. I. General concepts and the FCC to HCP transformation. Metall Trans A 1976;7:1897–1904.
14. Hornbogen E. Martensitic transformation at a propagating crack. Acta Metall 1978;26:147–152.
15. Garvie RC, Hannink RJH, Urbani C. Fracture mechanics study of a transformation toughened zirconia alloy in the CaO-ZrO_2 system. Ceram Int 1980;6:19–25.
16. Porter DL, Heuer AH. Mechanisms of toughening partially stabilized zirconia (PSZ). J Am Ceram Soc 1977;60:183–184.
17. Lange FF. Transformation toughening. I. Size effects associated with the thermodynamics of constrained transformations. J Mater Sci 1982;17:225–234.
18. Heuer AH, Claussen N, Kriven WM, Ruhle M. Stability of tetragonal ZrO_2 particles in ceramic matrices. J Am Ceram Soc 1982;65:642–650.
19. Swain MV, Garvie RC, Hannink RH. Influence of the thermal decomposition on the mechanical properties of magnesia-stabilized cubic zirconia. J Am Ceram Soc 1983;66:358–362.
20. Hannink RJ. Growth morphology of the tetragonal phase in partially stabilized zirconia. J Mater Sci 1978;13:2487–2496.
21. Evans AG, Cannon RM. Toughening of brittle solids by martensitic transformations. Acta Metall 1986;34:761–800.
22. Mei Z, Morris Jr JW. Influence of deformation-induced martensite on fatigue crack propagation in 304-type steels. Metall Trans A 1990;21:3137–3152.
23. Dauskardt RH, Marshall DB, Ritchie RO. Cyclic fatigue-crack propagation in magnesia-partially-stabilized zirconia ceramics. J Am Ceram Soc 1990;73:893–903.
24. McMeeking RM, Evans AG. Mechanics of transformation toughening in brittle materials. J Am Ceram Soc 1982;65:242–246.
25. Budiansky B, Hutchinson JW, Lambropoulos JC. Continuum theory of dilatent transformation toughening in ceramics. Int J Solids Struct 1983;19:337–355.
26. Rondelli G, Vicentini B, Cigada A. Corrosion properties of NiTi shape memory alloys. In: Otsuka K, Shimizu K, editors. Proceedings of MRS International Meeting on Advanced Materials. Vol. 9. Pittsburgh: Materials Research Society; 1989. p 237–242.
27. Suresh S. Fatigue of materials. New York: Cambridge University Press; 1991. 586 pp.
28. Boyce BL, Campbell JP, Roder O, Thompson AW, Milligan WW, Ritchie RO. Thresholds for high cycle fatigue in a turbine engine Ti-6Al-4V alloy. Int J Fatigue 1999; in press.
29. Pickard AC, Ritchie RO, Knott JF. Fatigue crack propagation in a type 316 stainless steel weldment. Metall Tech 1975;2:253–263.
30. Ritchie RO, Lubock P. Fatigue life estimation procedures for the endurance of a cardiac valve prosthesis: Stress/life and damage-tolerant analyses. J Biomed Eng 1986;108:153–160.
31. Li K, Thompson AW. Fatigue thresholds in titanium. Metall Trans A 1999; to appear.